

# Systemic tumor targeting and killing by Sindbis viral vectors

Jen-Chieh Tseng<sup>1</sup>, Brandi Levin<sup>1</sup>, Alicia Hurtado<sup>1</sup>, Herman Yee<sup>1</sup>, Ignacio Perez de Castro<sup>1</sup>, Maria Jimenez<sup>1</sup>, Peter Shamamian<sup>2</sup>, Ruzhong Jin<sup>3</sup>, Richard P Novick<sup>3</sup>, Angel Pellicer<sup>1</sup> & Daniel Meruelo<sup>1</sup>

**Successful cancer gene therapy requires a vector that systemically and specifically targets tumor cells throughout the body. Although several vectors have been developed to express cytotoxic genes via tumor-specific promoters or to selectively replicate in tumor cells, most are taken up and expressed by just a few targeted tumor cells. By contrast, we show here that blood-borne Sindbis viral vectors systemically and specifically infect tumor cells. A single intraperitoneal treatment allows the vectors to target most tumor cells, as demonstrated by immunohistochemistry, without infecting normal cells. Further, Sindbis infection is sufficient to induce complete tumor regression. We demonstrate systemic vector targeting of tumors growing subcutaneously, intrapancreatically, intraperitoneally and in the lungs. The vectors can also target syngeneic and spontaneous tumors in immune-competent mice. We document the anti-tumor specificity of a vector that systemically targets and eradicates tumor cells throughout the body without adverse effects.**

Two major obstacles to the development of gene therapy for cancer have been the inability to deliver gene therapy vectors systemically and specifically to primary and/or metastasized tumor cells without infecting normal tissues. Gene therapy vectors have been injected intratumorally; however, such treatments are generally not practical for patients with metastatic disease. Several viral vector systems have been developed to activate cytotoxic genes via tumor-specific promoters or to selectively replicate in tumor cells. When delivered systemically, however, only a small fraction of these vectors are taken up by the target tumors<sup>1–3</sup>. In such cases, tumor kill is generally insufficient to eradicate all tumor cells or substantially slow disease progress. We show here that Sindbis vectors may provide a solution to these and other obstacles.

Sindbis vectors were originally developed for efficient *in vitro* gene transfer to mammalian cells<sup>4</sup>. Several factors contribute to the vectors' potential utility for cancer gene therapy. First, Sindbis virus is a blood-borne virus that is transmitted to mammals by mosquito bites<sup>5</sup> and subsequently spreads throughout the body via the bloodstream<sup>6,7</sup>, where it has a relatively long half-life. Sindbis vectors, which are replication defective and safe<sup>8</sup>, retain the blood-borne attribute and are suitable for systemic administration. Second, the surface receptor on mammalian cells for Sindbis infection has been identified as the 67-kDa high-affinity laminin receptor (LAMR)<sup>9,10</sup>, which is substantially upregulated in numerous human cancers<sup>11–19</sup>. Higher expression of LAMR is related to the increasing invasiveness and malignancy of different cancers<sup>20,21</sup>, and, in contrast to normal cells, the majority of the LAMRs on cancer cells are not occupied by laminin<sup>22–24</sup>. High

levels of unoccupied LAMRs in tumor as compared to normal cells seem to confer on Sindbis vectors the ability to preferentially infect most tumor cells. Third, Sindbis vectors are well suited for tumor eradication because the infection is highly apoptotic in mammalian cells<sup>25–30</sup>. Our previous observations suggest that the vectors cause apoptosis of infected tumor cells *in vivo* without any cytotoxic gene payload<sup>8</sup>.

Here we used the IVIS Imaging System, a noninvasive system able to detect luciferase activity *in vivo*, to monitor successful delivery, infection and eradication of tumor cells by Sindbis vectors in live mice. We show that Sindbis vectors, regardless of injection route, target tumors growing subcutaneously (s.c.), intrapancreatically, intraperitoneally (i.p.) or in the lungs of C.B-17-SCID (SCID) mice. Sindbis vectors also target syngeneic and spontaneous tumors in immune-competent mice. Our findings indicate that, in addition to tumor eradication by vector infection, Sindbis vectors could be powerful tools for systemic detection of tumor metastases.

## RESULTS

### Sindbis/luc specifically infected subcutaneous BHK tumors

To test the potential of replication-defective Sindbis vectors for systemic delivery and tumor-specific infection, we injected a Sindbis/luc vector, containing a firefly luciferase gene, daily i.p. into SCID mice beginning when s.c. BHK tumors were approximately 500 mm<sup>3</sup> in size (day 1). The *in vivo* bioluminescence signals induced by vector infection were monitored using the IVIS Imaging System (Fig. 1). In treated mice, we observed tumor-specific bioluminescence on day 5 that

<sup>1</sup>New York University (NYU) Gene Therapy Center, NYU Cancer Institute and Department of Pathology, <sup>2</sup>Department of Surgery, and <sup>3</sup>Molecular Pathogenesis Program, Skirball Institute, Department of Microbiology and Department of Medicine, NYU School of Medicine, 550 First Avenue, New York, New York 10016, USA. Correspondence should be addressed to D.M. (daniel.meruelo@med.nyu.edu).

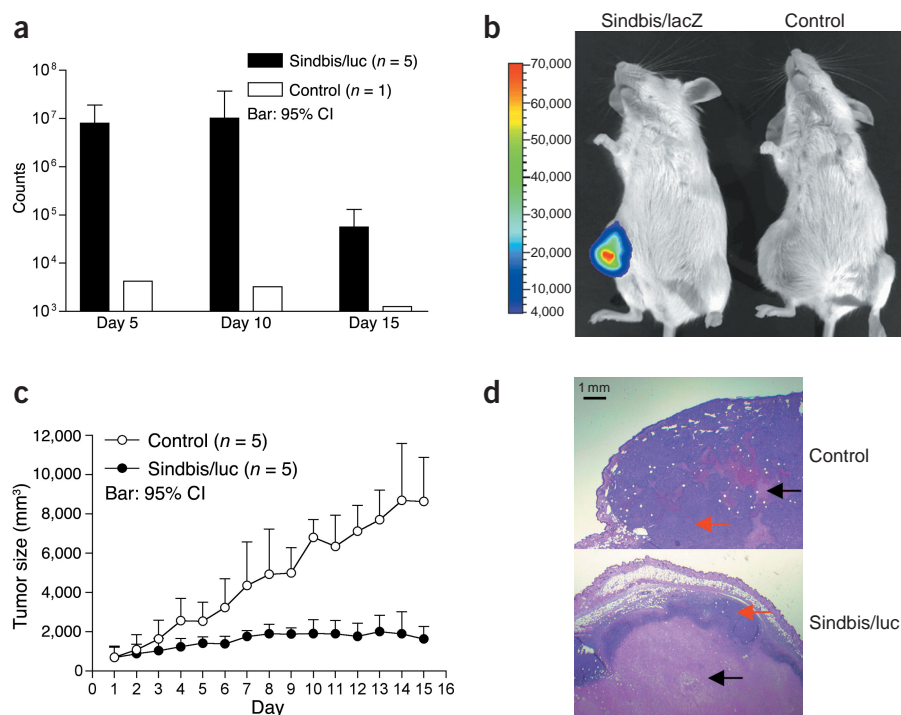


**Figure 1** Intra-peritoneal delivery of a Sindbis vector, Sindbis/luc, to S1CD mice bearing s.c. BHK tumors results in tumor-specific infection and tumor growth suppression. **(a)** Photon counts of s.c. BHK tumors treated with Sindbis/luc. Treated mice ( $n = 5$ ) showed tumor-specific bioluminescence signals, which dropped significantly on day 15 ( $P = 0.0038$ ); a control tumor-bearing mouse that did not receive vector treatment showed no bioluminescence signal. Bars, 95% confidence intervals. **(b)** Sindbis/luc vector treatment resulted in tumor-specific bioluminescence in treated BHK tumors and caused noticeable inhibition of tumor growth, as compared with untreated control tumor, on day 10. No substantial bioluminescence signal was seen in other regions. **(c)** Growth curves of s.c. BHK tumors treated with Sindbis/luc. The treatment significantly suppressed BHK tumor growth in mice treated with Sindbis/luc vectors ( $n = 5$ ) as compared with untreated control mice ( $n = 5$ ) ( $P < 0.0001$ , two-way ANOVA). Bar, 95% confidence intervals. **(d)** Intra-peritoneal Sindbis/luc treatment resulted in substantial size difference and extensive cell death in s.c. BHK tumors on day 15 after treatment. In BHK cross-sections stained with hematoxylin and eosin, purple hematoxyphilic regions (red arrows) designate viable tumor tissues and pink eosinophilic areas (black arrows) indicate necrotic tumor tissues. Tumors from control mice that received no Sindbis/luc treatment showed less cell death and a more irregular boundary between viable and necrotic tissues. In contrast, the Sindbis/luc-treated tumors showed extensive and homogenous tumor death except for the very outer rim.

persisted until day 10 but dropped significantly by day 15 (Fig. 1a). Untreated control s.c. BHK tumors generated very low background bioluminescence ( $\sim 10^3$  photon counts) as compared with Sindbis/luc-treated tumors ( $\sim 10^7$  photon counts). As demonstrated by the absence of bioluminescence signals in other regions of the treated mice (Fig. 1b), Sindbis/luc vectors specifically infected s.c. tumor cells.

#### Sindbis/luc caused tumor death and growth suppression

Statistical analysis of tumor sizes showed that Sindbis/luc vector completely suppressed the growth of s.c. tumors (Fig. 1c). We examined whether the reduction of bioluminescence signals and tumor growth resulted from tumor death induced by Sindbis-mediated apoptosis. Histopathology studies showed that this was the case: hematoxylin and eosin staining of tumor sections harvested on day 15 indicated that treated tumors had a much greater proportion of necrotic areas (pink regions) than did untreated control tumors (Fig. 1d). Furthermore, all of the treated tumors were homogeneously necrotic in a uniform radial appearance except at the very outer rims. In contrast, necrotic

areas in control tumors were smaller in size and more irregular in shape, as expected for necrosis resulting from tumor-associated phenomena such as hypoxia and poor nutrition. Our previous studies have indicated that s.c. tumors infected by Sindbis vectors regress completely within 3–4 weeks of treatment<sup>8</sup>.

#### Specific infection of intrapancreatic BHK SINLuc2 tumor

To determine whether Sindbis vectors can specifically infect BHK tumors growing at other locations, we established intrapancreatic tumors with a BHK-derived line, BHKSINLuc2, that stably transcribes a defective Sindbis replicon RNA containing a firefly luciferase gene<sup>31</sup>. Because this cell line expresses luciferase in response to Sindbis virus infection, we used BHKSINLuc2 tumors as biological reporters of vector infection. To reveal the distribution of vector infection within the pancreas, we used a Sindbis/lacZ vector that carries a bacterial  $\beta$ -galactosidase gene for subsequent immunohistochemical analysis. Intra-peritoneal inoculation of  $1 \times 10^6$  BHKSINLuc2 cells resulted in tumors mostly limited to the pancreas after 8 d. A single i.p. injection of Sindbis/lacZ led to specific infection of the intrapancreatic BHKSINLuc2 tumors and induction of luciferase activities (Fig. 2a, top). Without Sindbis/lacZ treatment, the control mice, bearing intrapancreatic BHKSINLuc2 tumor cells, showed no bioluminescence signal in the pancreas. The presence of tumors in the pancreas of both control and treated mice was confirmed by autopsy after imaging (Fig. 2a, bottom).

The IVIS Imaging System allows monitoring of vector infection events *in vivo*, and reflects the remarkable targeting capabilities of Sindbis vectors, confirmed by immunohistochemical analysis of the imaged mouse

(Fig. 2b). Tissue sections showed extensive tumor invasion of the pancreas (Fig. 2b, lower left; lighter areas of tissue section comprise tumor cells). Notably, after a single systemic administration of Sindbis/lacZ, most tumor cells within the pancreas stained positive for vector infection (Fig. 2b, lower right, brown areas), whereas normal cells did not; this is more evident at higher magnification (Fig. 2c, bottom). It is evident that areas of Sindbis infection are superimposable with tumor areas. These immunohistochemical pictures indicate why Sindbis vectors are effective at eradicating tumors: they infect and kill most tumor cells without affecting normal cells.

#### Sindbis/luc infected lung tumors via the bloodstream

To further confirm the ability of Sindbis vector to disseminate through the bloodstream for systemic detection, we used the IVIS Imaging System to determine specific vector targeting to tumors induced in the lungs. Intravenous inoculation of  $1 \times 10^6$  BHK cells results in growth of tumor cells in the lungs (Fig. 3). Seven days after inoculation, when mice showed tumor-related symptoms such as dyspnea, we injected

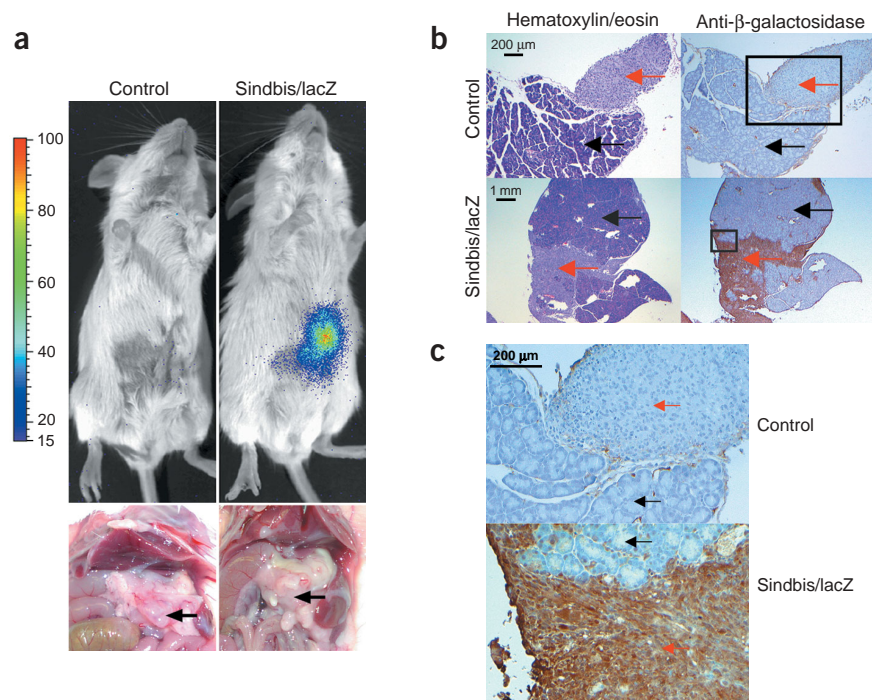


**Figure 2** Single i.p. delivery of Sindbis/lacZ vectors specifically infected intrapancreatic BHKSLuc2 tumors, which require Sindbis infection for luciferase gene expression. **(a)** Top, mice carrying an intrapancreatic BHKSLuc2 tumor showed substantial bioluminescence signal in the pancreas after single i.p. treatment with Sindbis/lacZ vectors. In contrast, control tumor-bearing mice that did not receive Sindbis/lacZ vectors showed no bioluminescence signal. Bottom, surgical examination at autopsy confirmed the presence of intrapancreatic BHKSLuc2 tumors in both control and Sindbis/lacZ-treated mice, as indicated by arrows. **(b)** Immunohistologic staining confirmed tumor-specific infection by Sindbis/lacZ vectors of intrapancreatic BHKSLuc2 tumors. Black and red arrows indicate normal pancreas tissue and BHKSLuc2 tumor cells, respectively. Consecutive sections (5  $\mu$ m apart) were stained with standard hematoxylin and eosin (left) or with a monoclonal antibody specific to the *lacZ* gene product, bacterial  $\beta$ -galactosidase (right), for immunohistologic staining. All BHKSLuc2 tumor regions within pancreas are positive for Sindbis/lacZ infection as determined by the brown  $\beta$ -galactosidase staining. **(c)** Boxed regions in **b** at higher magnification. Control slides show no positive  $\beta$ -galactosidase signal in either tumor or normal pancreas tissues. By contrast, strong  $\beta$ -galactosidase signals were detected exclusively in Sindbis/lacZ-treated tumor regions and formed a sharp border between tumor and normal pancreas tissues.

Sindbis/luc vectors i.v. for two consecutive days. Tumor-free control mice also received two Sindbis/luc treatments. On the day after the second Sindbis/luc treatment, we observed substantial bioluminescence signals in the chests of the BHK-injected mice but not the control mice (Fig. 3a). After imaging, lung metastases and tumor growth in BHK-injected mice were confirmed histologically (Fig. 3b).

#### Sindbis/luc detected micrometastatic i.p. ES-2 tumors

We determined the ability of Sindbis vectors to specifically infect microscopic tumors in our established mouse model of advanced ovarian cancer, which is induced by i.p. inoculation of ES-2 human ovarian cancer cells. Compared with normal mouse tissues, ES-2 cells express a higher level of *LAMR1*, which encodes the laminin receptor precursor (LRP), as determined by RT-PCR (Fig. 4a). Five days after i.p. inoculation of  $2 \times 10^6$  ES-2 cells, no gross tumor growth in the peritoneal cavity was visible except for few small (~2-mm), unattached tumor clusters (Fig. 4b). However, microscopic tumor metastases could be readily detected on the omentum, mesentery and diaphragm at this early stage of disease (Fig. 4c). Without any treatment, the mice developed grossly visible ascites and tumor growth on mesentery

and omentum within 2 weeks (Fig. 4b). A single i.p. injection of Sindbis/luc vectors in mice bearing microscopic ES-2 cancers for 5 d allowed the detection of bioluminescence signals on the omentum, mesentery and diaphragm (Fig. 4d).

#### Sindbis vectors suppressed advanced ovarian cancer

To study the therapeutic effects of Sindbis vectors, we derived ES-2/luc cells by stable transfection of a plasmid expressing the luciferase gene, so that we could track metastases *in vivo*. We were able to detect tumor metastasis the day after i.p. injection of  $1 \times 10^6$  ES-2/luc cells (Fig. 4e, day 1). Thus, as compared to gross and microscopic examination of mice, the use of ES-2/luc cells permitted earlier detection of microscopic tumor growth without the need for animal sacrifice.

To determine therapeutic effects, we started daily Sindbis treatments on day 1 with Sindbis/lacZ or Sindbis/IL-12 vectors. Sindbis vectors that carry mouse IL-12 genes have enhanced efficacy against s.c. tumors<sup>8</sup>. After four consecutive treatments, we observed significant reduction of tumor loads in Sindbis vector-treated mice. Tumor cells spread rapidly in the untreated SCID mice (Fig. 4e, top) but much more slowly in those treated with Sindbis vector (Fig. 4e, middle and bottom). The effect is clear with Sindbis/lacZ, but even more marked for mice treated with Sindbis/IL-12 (Fig. 4e, bottom). Total whole-body photon counts obtained from Sindbis/IL-12-treated mice show that by day 5 the treatments reduced the tumor load to 6.2% that of untreated control mice on average (Fig. 4f). In contrast, photon counts of untreated mice indicated that the number of cells by day 5 had increased 1.5-fold, to approximately  $1.5 \times 10^6$ , on average, and in some mice to  $2.3 \times 10^6$  cells. In the Sindbis/IL-12-treated mice, the number of cells declined to fewer than 90,000, on average, and in some mice to fewer than 23,000 cells (up to a 99% reduction of tumor cells as compared to untreated control mice). The same degree of inhibition was also observed at later time points (Fig. 4f). Injection of IL-12 alone without Sindbis vector was much less effective than Sindbis/IL-12 treatments and did not inhibit the formation of ascites, which subsequently began to develop in untreated mice but not in Sindbis vector-treated mice (data not shown).

#### Sindbis/luc infected s.c. Pan02 tumors in syngeneic mice

Because our previous models used immunodeficient mice to demonstrate specific tumor targeting, we tested whether the immune system presents a barrier to Sindbis tumor targeting in syngeneic tumor models. We induced s.c. tumors in C57BL/6 mice with Pan02 mouse pancreatic cancer cells and treated them daily with Sindbis/luc vectors. Pan02 cells also express higher levels of LAMR than normal cells (Fig. 4a). In mice, these cells form rapidly growing tumors that are highly resistant to all classes of chemotherapy agents<sup>32</sup>. However,

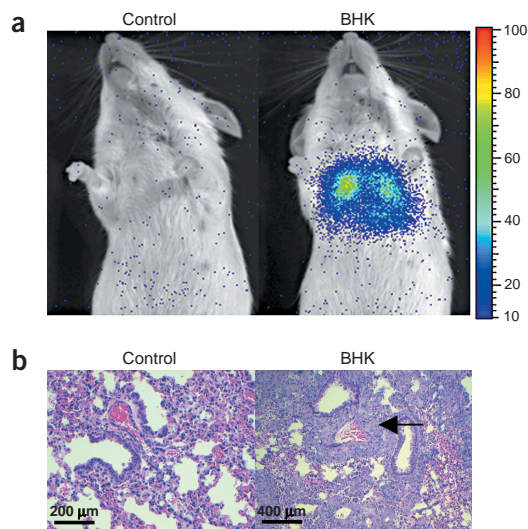


**Figure 3** Intravenous delivery of Sindbis/luc vectors targeted BHK tumors in the lung, which were induced by i.v. injection of BHK cells. **(a)** Intravenous injections of Sindbis/luc vector resulted in substantial bioluminescence signals in mice that carried BHK tumors in lungs. Tumor-free control mice showed no background bioluminescence signal. **(b)** Microscopically, the presence of BHK tumor cells in lung was confirmed by hematoxylin and eosin staining of lung sections obtained from tumor-free control or BHK-injected mice. The arrow indicates tumor cells in lung of a BHK-injected mouse. No tumor existed in the lungs of control mice.

Sindbis vectors can detect (Fig. 5a) and reduce the growth of s.c. Pan02 tumors (Fig. 5b;  $P < 0.0001$ , two-way ANOVA) in immunocompetent C57BL/6 mice. Despite the repeated administrations, the host immune response seems not to diminish the ability of the therapy to control tumor growth effectively. Also, we detected no evidence of adverse effects to the mice.

### Sindbis/luc specifically infected spontaneous tumors

To ensure that the preferential targeting by Sindbis for tumor cells is not due to their *in vitro* passage, we sought a spontaneous tumor model in an immunocompetent mouse, involving MSV-RGR/p15<sup>+/-</sup> transgenic mice, which are heterozygous for the *Rgr* oncogene and for the *Cdkn2b* gene, also known as *Ink4b* and *p15*. These mice develop spontaneous fibrosarcomas, particularly in the paws or tail. Because these tumors are not implanted or injected (Fig. 6a, left), they more closely mimic the physiological development of cancer. Results after Sindbis vector administrations show specific vector targeting to the tumors (Fig. 6a, right). All inoculations were done at sites on the mice as distant as possible from the tumors. We obtained photon counts from the tumor region on days 1, 4 and 14 (Fig. 6b). The intensity peaked on day 4, as vector accumulated at the tumor sites, and then diminished as the tumors became necrotic (Fig. 6c). This indicates that Sindbis vectors can target mouse tumors that arise spontaneously, while avoiding normal cells. The immune system seems not to diminish the ability of Sindbis/luc vectors to reach the tumor cells, as measured by imaging that was performed multiple times over a period of 2 weeks.

Notably, in the two immunocompetent mouse models described, only mouse cells are involved, whether they are normal or tumor. Thus, in all models depicted, whether human or mouse tumor cells are involved, Sindbis vectors specifically target tumor cells and do not infect normal cells. These results clearly indicate that the remarkable tumor

targeting specificity of the Sindbis vectors used in this study is not species dependent and that the antitumor activities of this vector system do not seem to be substantially obviated by the host immune system.

### DISCUSSION

Gene therapy for cancer would be greatly enhanced by the availability of a vector that could be delivered systemically and would have specific tumor targeting capability along with the ability to induce death in most primary and metastatic tumor cells. To specifically detect tumor cells, viral vector systems require either tumor-specific receptors for infection or, alternatively, the use of tumor-specific promoters for reporter transgene expression in tumor cells. In general, vectors using tumor-specific promoters for gene activation are taken up and expressed by only a small proportion of tumor cells, which is why they are unable to kill most metastases, and often have to be injected intratumorally. By contrast, vectors based on the Sindbis virus, which are highly apoptotic and infect via a ubiquitous receptor expressed differentially between tumor and normal cells, can target and kill tumor cells with very high efficacy. The cell surface receptor for Sindbis virus has been identified as the high-affinity LAMR<sup>9</sup>, a glycosylated membrane protein that mediates cellular interactions with the extracellular matrix and that is overexpressed and unoccupied (relative to normal cells) in the vast majority of tumors<sup>24,33–35</sup>. This characteristic also provides a differential marker on the surface of cells that provides a distinction between normal and tumor cells for Sindbis virus attachment and infection. In addition, Sindbis virus is naturally adapted to disseminate through the bloodstream. These two properties are largely responsible for our observation that systemic administration of replication-defective Sindbis vectors targets tumors growing s.c. (Figs. 1 and 5), intrapancreatically (Fig. 2), i.p. (Fig. 4) or in the lungs (Fig. 3). In addition, the apoptosis induced by vector infection explains why specific infection of tumor cells resulted in tumor death, growth inhibition and tumor regression<sup>8</sup>.

The Sindbis vectors we used in this study were derived from strain Toto1101 (ref. 4), which was generated after extensive passages of wild-type virus in mammalian cells. It has been proposed that heparan sulfate plays a role in the attachment of Toto1101 to cells<sup>36</sup>. However, although the interaction with heparan sulfate enhances infection efficiency, it is not required for infection<sup>36</sup>. If heparan-sulfated proteoglycan (HSPG) is part of the LAMR complex<sup>37,38</sup>, it is likely that, during extensive passage, the virus adapts to mammalian cells by acquiring mutations that enhance the interaction with heparan sulfate on the LAMR. Therefore, it is possible that the Sindbis vectors infect tumor cells via interactions with both LRP and heparan sulfate.

Our results here also demonstrate the ability of Sindbis viral vectors to specifically infect microscopic tumor metastases in the peritoneal cavity (Fig. 4c). The advantage of using viral gene therapy vectors for tumor detection is that the vector can markedly amplify the signals by overexpression of the transgene markers. Although luciferase expression might not be suitable for imaging of tumor cells in humans, because of the potentially greater depths at which such cells might be found in humans as compared to mice, other, more tissue-penetrating reporter genes can be incorporated into Sindbis vectors for tumor detection. For example, the herpes simplex virus type-1 thymidine kinase (HSV1-tk) and dopamine-2 receptor (D<sub>2</sub>R), which are suitable for detection by positron emission tomography (PET)<sup>39</sup>, can serve as reporters deliverable by gene therapy vectors.

Tumor detection and *in vivo* imaging using adenoviral vectors, with tumor-specific promoters for marker gene expression, have been reported<sup>40</sup>. Although tumor-specific promoters substantially reduce marker-gene expression in liver, these vectors are still found at high

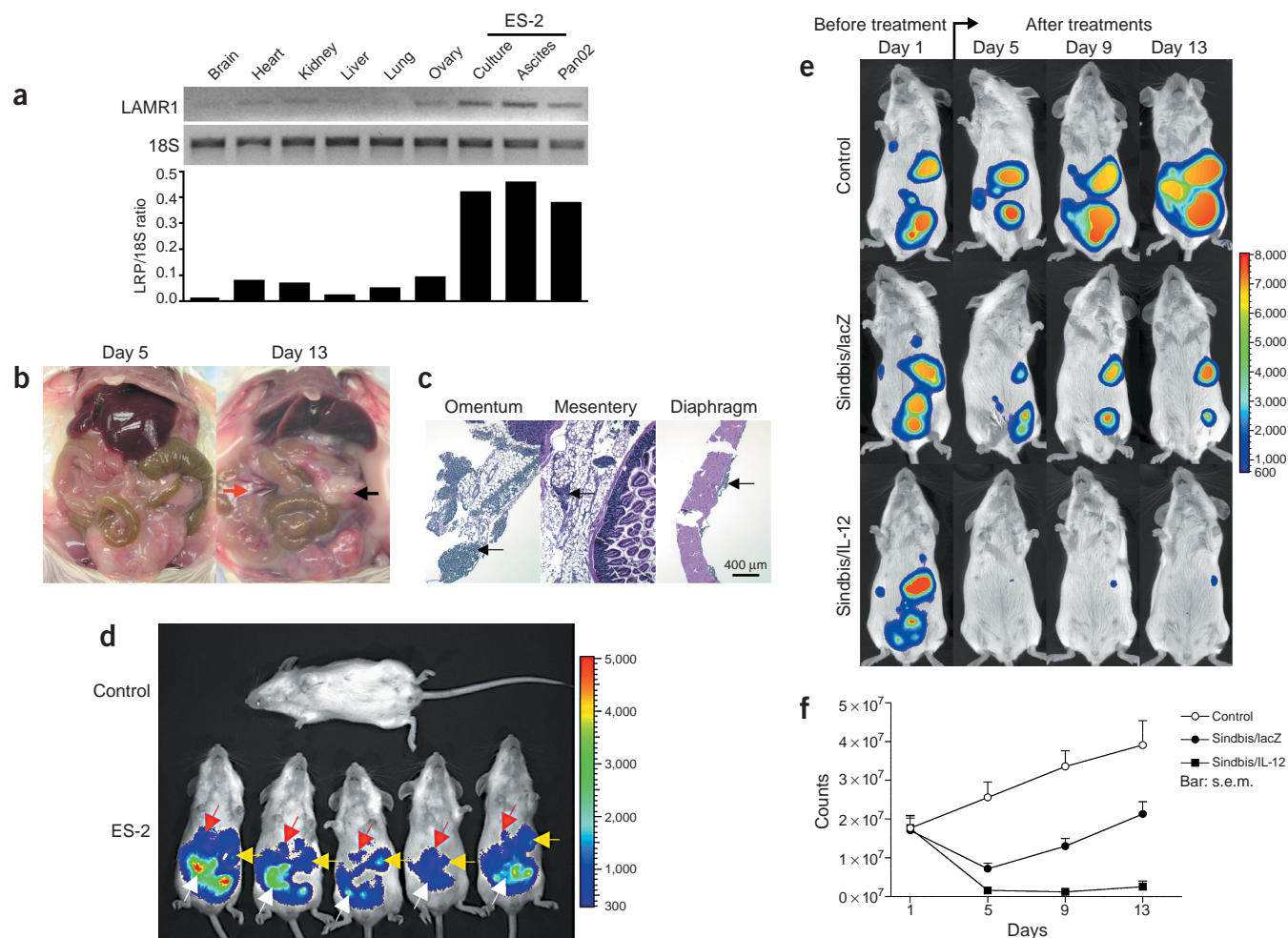


**Figure 4** Intraperitoneal treatment with Sindbis vectors specifically infected microscopic metastasized ES-2 ovarian tumors in the peritoneal cavity and significantly suppressed disease progress. **(a)** ES-2 and Pan02 cells highly express *LAMR1*. Top, total RNAs, isolated from organs of adult mice and from ES-2 and Pan02 cell cultures or ES-2 ascites, amplified by RT-PCR with primer pairs specific to the *LAMR1* transcript or 18S rRNA. Bottom, pixel intensity ratios of *LAMR1* RT-PCR signal to 18S RT-PCR signal. **(b)** Five days after i.p. inoculation of ES-2 cells, no grossly visible tumor metastasis is detected in the peritoneal cavities. However, 13 d after inoculation, tense ascites and extensive tumor growth can be grossly observed on the omentum (black arrow), mesentery (red arrow) and diaphragm. **(c)** Five days after ES-2 inoculation, microscopic metastasized ES-2 tumors (indicated by arrows) were observed in omentum, mesentery and diaphragm. **(d)** Five days after i.p. ES-2 inoculation, while the tumor growth was still microscopic, a single i.p. treatment of Sindbis/luc vectors specifically infected metastasized ES-2 cells and allowed their detection, 1 d later, on omentum (yellow arrows), mesentery (white arrows) and diaphragm (red arrows). Tumor-free control mice showed no substantial bioluminescence signal after receiving a Sindbis/luc. **(e)** SCID mice inoculated with ES-2/luc cells, which stably express luciferase activities, treated daily i.p. with Sindbis/lacZ or Sindbis/IL-12 vectors and imaged on days 1, 5, 9 and 13 after inoculation. Control mice received no vector treatment. Both Sindbis treatments significantly suppressed tumor growth on the mesentery and diaphragm, and reduced the signals on the omentum. The signals by the left legs at the lower abdomens were intramuscular tumors at tumor inoculation sites. **(f)** Quantitative analysis of the whole-body total photon counts of control and Sindbis vector-treated mice ( $P < 0.0001$ , two-way ANOVA).

levels in liver, raising concerns about potential liver toxicities<sup>40</sup>. Image development in this system seems to require many days. By contrast, because Sindbis vectors target only tumor cells and do so directly, within 1 d they yield robust expression of tumor-associated signals on most tumor cells (primary and metastases), providing faster and more sensitive detection without the need for tumor-specific promoters. No viral activity is seen in liver, heart, lung, kidney and testis tissues<sup>8</sup>, which is reflected in this study by the absence of vector infection signals in treated tumor-free mice.

Another potential advantage of these vectors is added safety, because they are replication-defective. In the vectors, the viral genome is split into one element comprising the replicon and reporter or therapeutic gene, and one or more elements comprising the structural

genes. Deleting the packaging signal from the helper RNA(s) encoding the structural genes ensures that these sequences are not packaged when vectors are shed from cells. Lacking structural genes, such vectors cannot generate new particles when they infect target cells. Although recombination can generate replication-competent vectors (RCV), this occurs with low frequency and can be screened for. In one configuration, the capsid and envelope glycoproteins were separated into distinct cassettes, resulting in vector packaging levels of  $10^7$  infectious units/ml, with contaminating RCV below the limit of detection<sup>41</sup>. The use of replication-defective, nonintegrating vectors precludes the development of viremia and introduces a safety level not available when RCVs are used for tumor therapy (although a number of approaches also have been suggested to rein in the risks of using RCVs<sup>42</sup>).

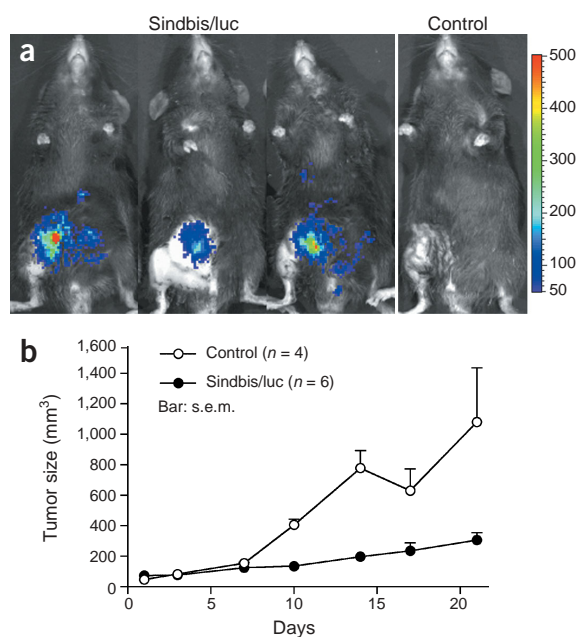


**Figure 5** Sindbis vector can target syngenic Pan02 s.c. tumor in immune-competent mouse. (a) Bioluminescence images of C57/BL/6 mice injected s.c. in the right hind flank with  $3 \times 10^6$  Pan02 cells suspended in 100  $\mu$ l of PBS on day 0, and then treated starting on day 6; imaging was done on day 7. Mice were randomly assigned to a control ( $n = 4$ ) and a Sindbis/luc vector group ( $n = 6$ ). (b) Growth curve of s.c. Pan02 tumors treated with Sindbis/luc vectors. Bar, s.e.m.

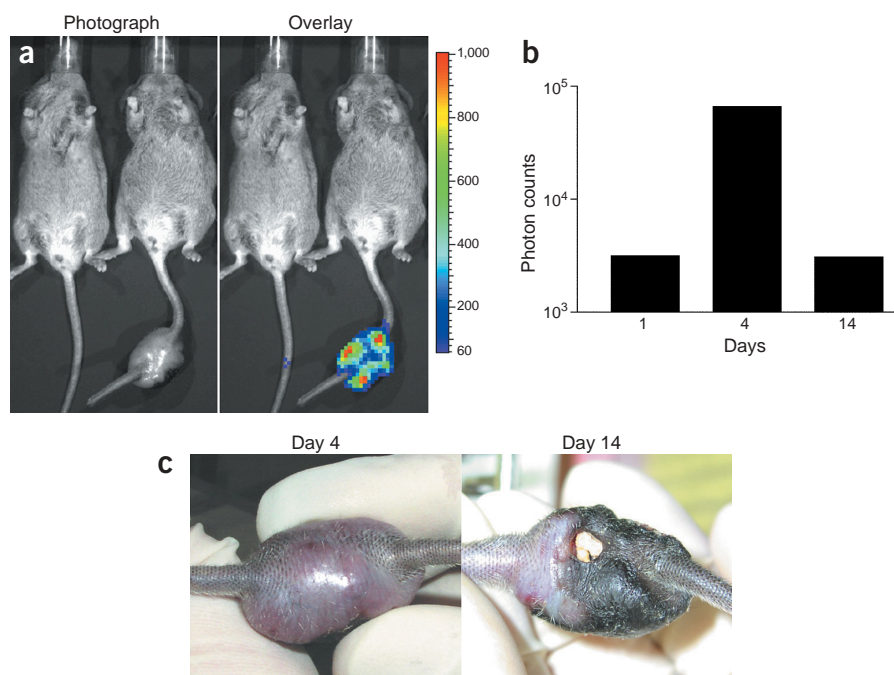


**Figure 6** Sindbis vector can target spontaneous tumors in *RGR/p15<sup>-/-</sup>* transgenic mice that develop tumors on the tail or paws. (a) A mouse bearing large tumors in the tail was treated i.p. with Sindbis/luc vectors for four consecutive days (started on day 0) and then imaged (day 4). Left, photograph of mice before imaging. Right, IVIS image overlay. (b) Photon counts of tail tumor on days 1, 4 and 14. (c) Tumor necrosis induced by Sindbis/luc infection after 2 weeks of treatments.

In conclusion, Sindbis vectors can achieve two major therapeutic goals of cancer gene therapy: specific marking of tumor cells, primary and metastatic, and efficient tumor suppression and eradication. Thus, Sindbis vectors seem to be potentially promising new agents for the treatment of cancer. Additional laboratory and clinical works will be required to investigate and develop the observations reported in this paper.

## METHODS

**Cells and vector preparation.** BHK, BHKSINLuc2 and ES-2 cells were obtained from the American Type Culture Collection (ATCC). BHK and BHKSINLuc2 cells were maintained in  $\alpha$ MEM (JRH Bioscience) with 5% FBS. The BHKSINLuc2 cells were derived from BHK cells and were stably transfected with a plasmid carrying a defective luciferase replicon under the control of a Rous sarcoma virus promoter<sup>31</sup>. ES-2 cells were derived from a patient with clear cell carcinoma, a type of ovarian cancer that has a poor prognosis and is resistant to several chemotherapeutic agents including cisplatin. ES-2 cells were cultured in McCoy's 5A medium (Mediatech) with 5% FBS. Pan02 cells were obtained from the NCI-Frederick Cancer Research Facility and were maintained in DMEM supplemented with 10% FBS. Pan02 is a highly tumorigenic pancreatic cancer cell line with ductal morphology that was derived from 3-methylcholanthrene (3-MCA)-induced tumors in C57BL/6 mice. All basal media were supplemented with 100  $\mu$ g/ml of penicillin-streptomycin and 0.5  $\mu$ g/ml of amphotericin B (both from Mediatech). ES-2/luc cells were derived from the ES-2 line by transfection of a plasmid, pIRES2-Luc/EGFP, that expresses a bicistronic mRNA transcript containing both firefly luciferase and EGFP genes. To construct the pIRES2-Luc/EGFP plasmid, a DNA fragment containing the luciferase gene was obtained from pGL-3 basic plasmid (Promega) and then subcloned into the multicloning sites of the pIRES2-EGFP plasmid (BD Biosciences Clontech).

Sindbis vectors (Sindbis/luc, Sindbis/lacZ and Sindbis/IL-12) were produced as described previously<sup>8</sup>. Briefly, the plasmids carrying the Sindbis replicon (SinRep/Luc, SinRep/LacZ or SinRep/IL-12) or DHBB helper RNAs were linearized with *NotI* or *XhoI*, respectively, before *in vitro* transcription using the mMESSAGE mMACHINE RNA transcription kit (SP6 version; Ambion). Both helper and replicon RNA transcripts (20  $\mu$ l each) were then electroporated into BHK cells and incubated in 10 ml of  $\alpha$ MEM containing 5% FBS at 37  $^{\circ}$ C for 12 h. The medium was replaced with 10 ml of Opti-MEM I medium (GIBCO-BRL). After 24 h, culture medium was collected and stored at -80  $^{\circ}$ C. The titers of Sindbis vectors were determined as described previously<sup>8</sup>.

**Measurement of *LAMR1* transcripts by RT-PCR.** Using the RNeasy Mini Kit (Qiagen), total RNA was isolated from ES-2 and Pan02 cell culture and from ES-2 ascites obtained from a SCID mouse (Taconic) 14 d after intraperitoneal ES-2 inoculation. Total mouse RNA from different tissues, such as brain, heart, kidney, liver, lung and ovary, were purchased from Ambion. The *LAMR1* transcript levels in different tissues were compared by reverse transcription polymerase chain reaction (RT-PCR) with a primer pair specific to *LAMR1* mRNA: sense 5'-CACAAATGTCCGGAGCCCTTG-3', antisense 5'-AGCAGCAAACCTTCAGCACAG-3'. 12.5 ng of total RNA was used for *LAMR1* RT-PCR and the predicted product size was 280 bp. Both primers are completely homologous to both the human and mouse *LAMR1* genes, with the sense primer located in the first exon and the antisense primer in the third exon to avoid unwanted genomic DNA amplification. Parallel RT-PCR using QuantumRNA universal 18S primers (Ambion) as a loading control

was also performed. Because of the relative abundance of 18S rRNA in the RNA samples, the universal primers were mixed with their competitors (primer/competitor ratio = 4:6) before amplification. 12.5 ng of total RNA was amplified and the predicted 18S band size was 315 bp. RT-PCR reactions were performed following the manufacturer's instruction with the SuperScript one-step RT-PCR with Platinum *Taq* system (Invitrogen). The total reaction volume was 50  $\mu$ l. After 30 min incubation at 45 °C for first-strand synthesis, the cDNA was amplified for 40 cycles, with each cycle consisting of 94 °C  $\rightarrow$  59 °C  $\rightarrow$  72 °C transitions. 15  $\mu$ l of the RT-PCR products were separated on 2% agarose gels and visualized after staining with ethidium bromide. The band pixel intensities on the agarose gel were calculated using NIH Image version 1.63 (National Institutes of Health, Bethesda, Maryland). The pixel intensity ratios of corresponding RT-PCR bands in different tissues were calculated with the formula: (LAMP1 band pixel intensity)/(18S rRNA band pixel intensity).

**Animal models.** All animal experiments were done in accordance with NIH and institutional guidelines. To induce s.c. tumors,  $1 \times 10^6$  BHK cells were injected s.c. in the right flank of the lower abdomen of SCID mice (female, 6–8 week old; Taconic). After 12 d, when the BHK tumors had reached a size of at least 500 mm<sup>3</sup>, the mice were randomly assigned to a control ( $n = 5$ ) and a Sindbis/luc ( $n = 5$ ) group, and the treatment was started on that day (day 1). The Sindbis/luc group received daily i.p. injections on the left flank of the lower abdomen consisting of 0.5 ml of Opti-MEM I containing  $10^7$ – $10^8$  CFU of Sindbis/luc vectors. Control mice received 0.5 ml of Opti-MEM I. Bioluminescence in mice was monitored on days 5, 10 and 15 using the IVIS Imaging System Series 100 (see below for details of detection procedure). The size of BHK tumors was determined daily with caliper using the formula (length, mm)  $\times$  (width, mm)  $\times$  (height, mm). Tumor size data was statistically analyzed with two-way ANOVA using GraphPad Prism version 3.0a for Macintosh (GraphPad Software) as described previously<sup>8</sup>.

To induce intrapancreatic tumors, SCID mice were anesthetized and then injected intrapancreatically with  $1 \times 10^6$  BHKSINLuc2 cells using 21-gauge syringes. Eight days later, 0.5 ml Sindbis/lacZ vectors ( $\sim 10^7$  CFU) was injected i.p. into mice bearing BHKSINLuc tumors. The next day, the mice were monitored for bioluminescence using the IVIS Imaging System. Mice were euthanized the day after imaging to document tumor growth photographically.

To obtain lung tumors,  $1 \times 10^6$  BHK cells were injected via the tail vein. Seven days later, mice were injected with 0.5 ml Sindbis/luc vectors ( $\sim 10^7$  CFU) via the tail vein for two consecutive days. Tumor-free control mice were treated with Sindbis/luc vector in parallel. The day after the second injection we monitored luciferase activity within mice using the IVIS Imaging System. We euthanized the mice the day after imaging and documented tumor growth photographically and histologically (see below).

To establish the advanced ovarian cancer model, female SCID mice were injected i.p. with  $2 \times 10^6$  ES-2 cells in 0.5 ml DMEM supplemented with 10% FBS. To determine tumor-specific infection of Sindbis vectors, mice were treated with single i.p. injection of Sindbis/luc 5 d after ES-2 inoculation, and the *in vivo* bioluminescence of tumor cells was determined using the IVIS Imaging System.

To determine the therapeutic efficacy of Sindbis vectors, SCID mice were injected with  $1 \times 10^6$  ES-2/luc cells on day 0 and imaged with the IVIS system the next day (day 1). The mice then received daily i.p. treatments of Sindbis/lacZ ( $n = 5$ ) or Sindbis/IL-12 ( $n = 5$ ) ( $\sim 10^7$  CFU in 0.5 ml Opti-MEM I) and were imaged with the IVIS system on days 5, 9 and 13. Control mice ( $n = 5$ ) received no Sindbis treatment.

Female C57/BL/6 mice 6–8 weeks of age were injected s.c. in the right hind flank with  $3 \times 10^6$  Pan02 cells suspended in 100  $\mu$ l of PBS on day 0. Six days later the mice were randomly assigned to a control ( $n = 4$ ) and a Sindbis/luc ( $n = 6$ ) group, and the treatment was started on that day (day 6). The next day (day 7) all mice were imaged with the IVIS system. From then on the size of Pan02 tumors was determined twice a week with caliper.

MSV-RGR/p15<sup>+/-</sup> offspring were generated as littermates of MSV-RGR and KO-p15 mice. M. Jimenez, I. Perez de Castro and A. Pellicer generated MSV-RGR transgenic mice in one of our laboratories. Briefly, an *Rgr* transgene, consisting of *Rgr* cDNA regulated by a Moloney murine sarcoma virus (MSV) promoter, was injected into the pronucleus of fertilized eggs from female (FVB/N) donors and later transferred to pseudopregnant mice. All the

MSV-RGR/p15<sup>+/-</sup> mice developed fibrosarcomas in the limbs, tail and/or ears, as compared to only 5–10% of the MSV-RGR mice. MSV-RGR/p15<sup>+/-</sup> carrying limb or tail tumors received daily i.p. treatments of Sindbis/luc on day 0 and were imaged on days 2, 4 and 14. Tumor-free control mice received Sindbis/luc treatments and were imaged in parallel.

***In vivo* bioluminescence detection with the IVIS Imaging System.** We used a cryogenically cooled IVIS Imaging System Series 100 (Xenogen) with Living Image acquisition and analysis software (Version 2.11, Xenogen) to detect the bioluminescence signals in mice. Each mouse was injected i.p. with 0.3 ml of 15 mg/ml beetle luciferin (potassium salt; Promega) in PBS. After 5 min, mice were anesthetized with 0.3 ml of avertin (1.25% of 2,2,2-tribromoethanol in 5% *tert*-amyl alcohol) or isofluran-mixed oxygen. The imaging system first took a photographic image in the chamber under dim illumination; this was followed by luminescent image acquisition. The overlay of the pseudocolor images represents the spatial distribution of photon counts produced by active luciferase. An integration time of 1 min was used for luminescent image acquisition for all mouse tumor models. We use Living Image software to integrate the total bioluminescence signals (in terms of photon counts) obtained from mice. The *in vitro* detection limit of the IVIS Imaging System is  $\sim 1,000$  ES-2/luc cells.

**Histological analysis and immunohistological staining.** Tissues were fixed in 10% neutral buffered formalin for at least 12 h, routinely processed and then embedded in paraffin. Tissue sections of 5  $\mu$ m were prepared on electrostatically charged glass slides and then baked at 60 °C overnight. After deparaffinization with three washes in xylene, the sections were rehydrated through a series of graded ethanols (100%, 90% and 70%) to water before staining with hematoxylin and eosin. Hematoxyphilic stained areas (purple regions) are areas of viable tumor while eosinophilic areas (pink regions) indicate nonviable areas. To detect specific tumor infection by Sindbis/lacZ vector of intrapancreatic tumors, we carried out immunohistochemical staining on pancreas sections with a mouse monoclonal antibody specific to the *lacZ* gene product, bacterial  $\beta$ -galactosidase (clone 2E9; 1:20 dilution; BioDesign International), as described previously<sup>8</sup>.

#### ACKNOWLEDGMENTS

We thank Elizabeth W. Newcomb, Christine Pampeno and Colby Collier for critical reading of this manuscript and helpful discussions. This study was supported by US Public Health Service grants CA22247 and CA68498 from the National Cancer Institute, National Institutes of Health, Department of Health and Human Services, by U.S. Army grant 0C000111 and by a generous gift from the Karan-Weiss Foundation.

#### COMPETING FINANCIAL INTERESTS

The authors declare that they have no competing financial interests.

Received 1 October; accepted 29 October 2003

Published online at <http://www.nature.com/naturebiotechnology/>

1. Akporiaye, E.T. & Hersh, E. Clinical aspects of intratumoral gene therapy. *Curr. Opin. Mol. Ther.* **1**, 443–453 (1999).
2. Green, N.K. & Seymour, L.W. Adenoviral vectors: systemic delivery and tumor targeting. *Cancer Gene Ther.* **9**, 1036–1042 (2002).
3. Biederer, C., Ries, S., Brandts, C.H. & McCormick, F. Replication-selective viruses for cancer therapy. *J. Mol. Med.* **80**, 163–175 (2002).
4. Bredenbeek, P.J., Frolov, I., Rice, C.M. & Schlesinger, S. Sindbis virus expression vectors: packaging of RNA replicons by using defective helper RNAs. *J. Virol.* **67**, 6439–6446 (1993).
5. Strauss, J.H. & Strauss, E.G. The alphaviruses: gene expression, replication, and evolution. *Microbiol. Rev.* **58**, 491–562 (1994).
6. Ryman, K.D., Klimstra, W.B., Nguyen, K.B., Biron, C.A. & Johnston, R.E.  $\alpha\beta$  interferon protects adult mice from fatal Sindbis virus infection and is an important determinant of cell and tissue tropism. *J. Virol.* **74**, 3366–3378 (2000).
7. Cook, S.H. & Griffin, D.E. Luciferase imaging of a neurotropic viral infection in intact animals. *J. Virol.* **77**, 5333–5338 (2003).
8. Tseng, J.C. *et al.* *In vivo* antitumor activity of Sindbis viral vectors. *J. Natl. Cancer Inst.* **94**, 1790–1802 (2002).
9. Wang, K.S., Kuhn, R.J., Strauss, E.G., Ou, S. & Strauss, J.H. High-affinity laminin receptor is a receptor for Sindbis virus in mammalian cells. *J. Virol.* **66**, 4992–5001 (1992).
10. Strauss, J.H., Wang, K.S., Schmaljohn, A.L., Kuhn, R.J. & Strauss, E.G. Host-cell receptors for Sindbis virus. *Arch. Virol. Suppl.* **9**, 473–484 (1994).

11. Martignone, S. *et al.* Prognostic significance of the 67-kilodalton laminin receptor expression in human breast carcinomas. *J. Natl. Cancer Inst.* **85**, 398–402 (1993).
12. Sanjuan, X. *et al.* Overexpression of the 67-kD laminin receptor correlates with tumour progression in human colorectal carcinoma. *J. Pathol.* **179**, 376–380 (1996).
13. de Manzoni, G. *et al.* Study on Ki-67 immunoreactivity as a prognostic indicator in patients with advanced gastric cancer. *Jpn. J. Clin. Oncol.* **28**, 534–537 (1998).
14. Tarabozetti, G., Belotti, D., Giavazzi, R., Sobel, M.E. & Castronovo, V. Enhancement of metastatic potential of murine and human melanoma cells by laminin receptor peptide G: attachment of cancer cells to subendothelial matrix as a pathway for hematogenous metastasis. *J. Natl. Cancer Inst.* **85**, 235–240 (1993).
15. Ozaki, I. *et al.* Differential expression of laminin receptors in human hepatocellular carcinoma. *Gut* **43**, 837–842 (1998).
16. van den Brule, F.A. *et al.* Expression of the 67 kD laminin receptor in human ovarian carcinomas as defined by a monoclonal antibody, MLu5. *Eur. J. Cancer* **32A**, 1598–1602 (1996).
17. van den Brule, F.A. *et al.* Differential expression of the 67-kD laminin receptor and 31-kD human laminin-binding protein in human ovarian carcinomas. *Eur. J. Cancer* **30A**, 1096–1099 (1994).
18. Liebman, J.M., Burbelo, P.D., Yamada, Y., Fridman, R. & Kleinman, H.K. Altered expression of basement-membrane components and collagenases in ascitic xenografts of OVCAR-3 ovarian cancer cells. *Int. J. Cancer* **55**, 102–109 (1993).
19. Ciocce, V. *et al.* Increased expression of the laminin receptor in human colon cancer. *J. Natl. Cancer Inst.* **83**, 29–36 (1991).
20. Menard, S., Tagliabue, E. & Colnaghi, M.I. The 67 kDa laminin receptor as a prognostic factor in human cancer. *Breast. Cancer. Res. Treat.* **52**, 137–145 (1998).
21. Viacava, P. *et al.* The spectrum of 67-kD laminin receptor expression in breast carcinoma progression. *J. Pathol.* **182**, 36–44 (1997).
22. Liotta, L.A. Tumor invasion and metastases—role of the extracellular matrix: Rhoads Memorial Award lecture. *Cancer Res.* **46**, 1–7 (1986).
23. Aznavoorian, S., Murphy, A.N., Stetler-Stevenson, W.G. & Liotta, L.A. Molecular aspects of tumor cell invasion and metastasis. *Cancer* **71**, 1368–1383 (1993).
24. Liotta, L.A., Rao, N.C., Barsky, S.H. & Bryant, G. The laminin receptor and basement membrane dissolution: role in tumour metastasis. *Ciba Found. Symp.* **108**, 146–162 (1984).
25. Levine, B. *et al.* Conversion of lytic to persistent alphavirus infection by the bcl-2 cellular oncogene. *Nature* **361**, 739–742 (1993).
26. Jan, J.T., Chatterjee, S. & Griffin, D.E. Sindbis virus entry into cells triggers apoptosis by activating sphingomyelinase, leading to the release of ceramide. *J. Virol.* **74**, 6425–6432 (2000).
27. Jan, J.T. & Griffin, D.E. Induction of apoptosis by Sindbis virus occurs at cell entry and does not require virus replication. *J. Virol.* **73**, 10296–10302 (1999).
28. Balachandran, S. *et al.*  $\alpha/\beta$  interferons potentiate virus-induced apoptosis through activation of the FADD/caspase-8 death signaling pathway. *J. Virol.* **74**, 1513–1523 (2000).
29. Frolov, I. & Schlesinger, S. Comparison of the effects of Sindbis virus and Sindbis virus replicons on host cell protein synthesis and cytopathogenicity in BHK cells. *J. Virol.* **68**, 1721–1727 (1994).
30. Frolova, E.I. *et al.* Roles of nonstructural protein nsP2 and  $\alpha/\beta$  interferons in determining the outcome of Sindbis virus infection. *J. Virol.* **76**, 11254–11264 (2002).
31. Olivo, P.D., Frolov, I. & Schlesinger, S. A cell line that expresses a reporter gene in response to infection by Sindbis virus: a prototype for detection of positive strand RNA viruses. *Virology* **198**, 381–384 (1994).
32. Putzer, B.M., Rodicker, F., Hitt, M.M., Stiewe, T. & Esche, H. Improved treatment of pancreatic cancer by IL-12 and B7.1 costimulation: antitumor efficacy and immunoregulation in a nonimmunogenic tumor model. *Mol. Ther.* **5**, 405–412 (2002).
33. Liotta, L.A. *et al.* Monoclonal antibodies to the human laminin receptor recognize structurally distinct sites. *Exp. Cell Res.* **156**, 117–126 (1985).
34. Barsky, S.H., Rao, C.N., Hyams, D. & Liotta, L.A. Characterization of a laminin receptor from human breast carcinoma tissue. *Breast Cancer Res. Treat.* **4**, 181–188 (1984).
35. Terranova, V.P., Rao, C.N., Kalebic, T., Margulies, I.M. & Liotta, L.A. Laminin receptor on human breast carcinoma cells. *Proc. Natl. Acad. Sci. USA* **80**, 444–448 (1983).
36. Byrnes, A.P. & Griffin, D.E. Binding of Sindbis virus to cell surface heparan sulfate. *J. Virol.* **72**, 7349–7356 (1998).
37. Leucht, C. *et al.* The 37 kDa/67 kDa laminin receptor is required for PrP(Sc) propagation in scrapie-infected neuronal cells. *EMBO Rep.* **4**, 290–295 (2003).
38. Gauczynski, S. *et al.* The 37-kDa/67-kDa laminin receptor acts as the cell-surface receptor for the cellular prion protein. *EMBO J.* **20**, 5863–5875 (2001).
39. Yaghoubi, S.S. *et al.* Direct correlation between positron emission tomographic images of two reporter genes delivered by two distinct adenoviral vectors. *Gene Ther.* **8**, 1072–1080 (2001).
40. Adams, J.Y. *et al.* Visualization of advanced human prostate cancer lesions in living mice by a targeted gene transfer vector and optical imaging. *Nat. Med.* **8**, 891–897 (2002).
41. Polo, J.M. *et al.* Stable alphavirus packaging cell lines for Sindbis virus and Semliki Forest virus-derived vectors. *Proc. Natl. Acad. Sci. USA* **96**, 4598–4603 (1999).
42. Antonio Chioocca, E. Oncolytic viruses. *Nat. Rev. Cancer* **2**, 938–950 (2002).